

# Electrochemical studies of laser-treated Co–Cr–Mo alloy in a simulated physiological solution

R. A. SILVA

*INEB–Instituto de Engenharia Biomedica/ISEP–Instituto Politécnico do Porto, Rua de S. Tomé, 4200 Porto, Portugal*

M. A. BARBOSA

*INEB–Instituto de Engenharia Biomedica/FEUP–Faculdade de Engenharia da Universidade do Porto, Portugal*

R. VILAR

*IST, Technical University of Lisbon, Portugal*

O. CONDE

*Faculty of Sciences, Department of Physics, University of Lisbon, Portugal*

M. DA CUNHA BELO

*CECM-CNRS, Vitry/Seine, France*

I. SUTHERLAND

*Department of Chemistry, Loughborough University of Technology, UK*

The aims of this work were to study the crevice corrosion resistance of laser-treated Co–Cr–Mo alloy by electrochemical techniques and to characterize the electronic properties of the passivating films. Open-circuit experiments and cyclic polarizations with crevice-free samples have been carried out as well as electrochemical impedance spectra using Bode–Nyquist and Mott–Schottky techniques. Scanning electron microscopy (SEM) and X-ray photoelectron spectroscopy (XPS) analysis have been used in order to evaluate surface modifications. It has been observed that laser-treated Co–Cr–Mo alloy shows good corrosion resistance in spite of some degradation at the dendrites formed during treatment. By XPS it was found that at 6–9 nm depth there exists an enrichment in oxygen and a decrease of Cr which could have a slight effect on the corrosion resistance and it was seen that the film is mostly formed by  $\text{Cr}_2\text{O}_3$ . Mott–Schottky plots show that a possible transition from n-type to p-type semiconductivity may have occurred.

## 1. Introduction

Co–Cr–Mo alloys are widely used as orthopaedic devices because of their corrosion resistance [1–2]. Nevertheless, there exists always a residual current that leads to the release of metallic ions to the adjacent tissues of the prosthesis that may provoke systemic reactions as infections or allergies. These processes may be associated with the presence of carbide precipitates in the grain boundaries [3]. On the other hand, the technology of fabrication of Co alloys results in small voids on the surfaces that, in terms of mechanical properties, may have some deleterious effects.

The present work was aimed at evaluating, by electrochemical means, the effect of laser treatment on the corrosion resistance of Co alloys, considering that the elimination of carbide precipitates and voids could improve both corrosion and mechanical properties of the material.

## 2. Experimental methods

The experiments were carried out with Co–Cr–Mo alloy (C-0.38%, S-0.009%, Fe-0.37%, Mo-5.35%, Cr-29.83% wt/wt) electrodes with a diameter of 10 mm and a thickness of 2 mm, as received. Before laser treatment, the electrodes were polished down to 600 grit SiC paper and then degreased ultrasonically in trichloroethylene and acetone and finally rinsed in deionized water. After laser treatment, and 24 h before testing, the electrodes were polished with 1  $\mu\text{m}$  diamond paste and cleaned again as described before.

The laser treatment was performed using a  $\text{CO}_2$  Coherent Everlaser 548 instrument with maximum power of 800 W. The power required for melting the material did not exceed 200 W. The samples were submitted to multiple pass scanning with partial (ca 50%) superposition of consecutive tracks. To avoid oxidation, the surface was protected with a nitrogen jet, coaxial with the laser beam.

Open-circuit corrosion tests with crevice geometry were carried out in a cell with four windows under the conditions described elsewhere [4, 5]. For the cyclic polarization experiments crevice-free specimens were mounted according to the methodology described in [6], and in order to carry out the impedance tests preparation of the electrodes was performed as described in [7]. The composition of the solution was, in mM:  $\text{Na}^+$  137,  $\text{K}^+$  4,  $\text{Ca}^{2+}$  6.6,  $\text{Mg}^{2+}$  5.0,  $\text{Cl}^-$  110, acetate 36.8;  $\text{pH} = 6.7$ . Continuous monitoring of the open-circuit corrosion potential was carried out for 6 days using a channel selector (Cole-Parmer model 8388) and a digital pH millivoltmeter (Philips PW 9409). Cyclic polarization curves were conducted at a sweep rate of  $50 \text{ mV min}^{-1}$ , at room temperature, using a Tacussel Potentiostat PRT-20-2X. A standard polarization cell (ASTM G5-78 standard) was used.

The solution was deaerated with  $\text{N}_2$ . Electrochemical impedance Bode diagrams ( $\log |Z|$  versus  $\log \bar{\omega}$ ) were drawn for films formed under open-circuit conditions. The tests were carried out at rest potential. The frequency was varied from  $5 \times 10^{-3} \text{ Hz}$  to 100 kHz. For the higher values of frequency the measurements were made with a lock-in amplifier (EG&G M 5208) coupled to a potentiostat (EG&G M 273). For the lower frequency range a fast Fourier Transform (FFT) algorithm was used.

Mott-Schottky plots were obtained using the same system. The specimens were polarized from  $-0.4 \text{ V}$  to  $+0.4 \text{ V}$  at a potential sweep rate of  $30 \text{ mV min}^{-1}$  at constant frequency (1 kHz). A Saturated Calomel Electrode (SCE) was used for all electrochemical studies. A Pt foil or wire served as auxiliary electrode in the potentiokinetic and impedance tests, respectively.

Electron spectra were recorded on a VG scientific Escalab spectrometer with dual (Mg/Al) X-ray anode. Binding energies were referenced to Cls at 284.6 eV. Compositions were determined taking into account the photoelectron cross-sections, inelastic mean free path, angular asymmetry in photoemission and the transmission of the energy analyser.

### 3. Results and discussion

Fig. 1 shows the dendrites formed in Co-Cr-Mo alloy after laser treatment, and Fig. 2 shows the laser

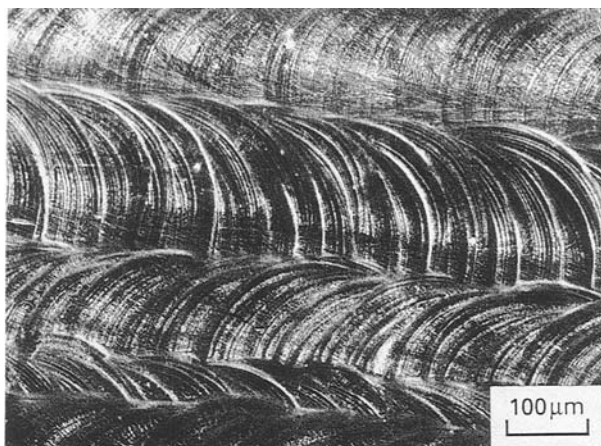


Figure 1 Dendrites formed during cooling of the material.

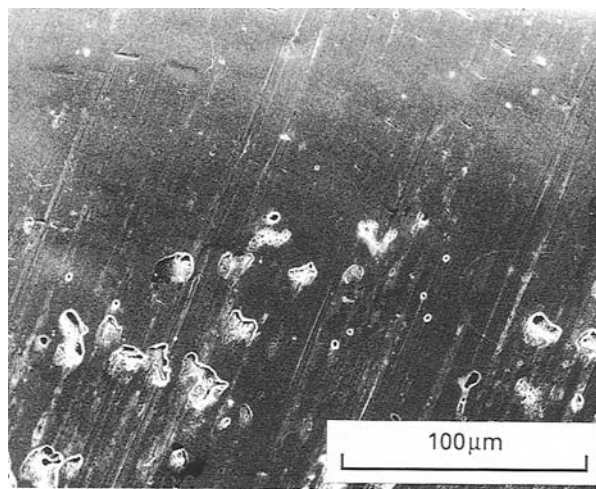


Figure 2 Co alloy surface after laser treatment.

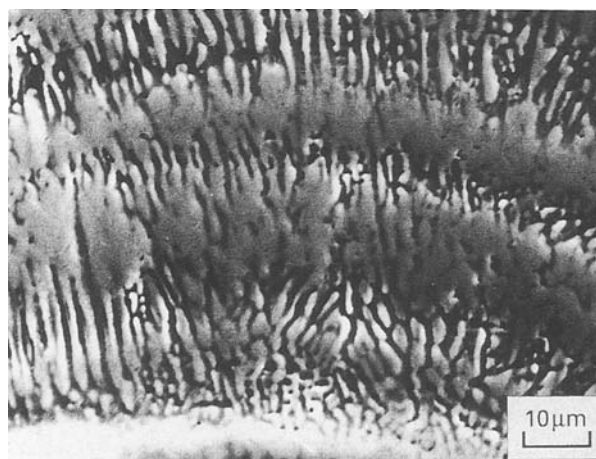


Figure 3 Presence of voids at a depth of 100  $\mu\text{m}$ .

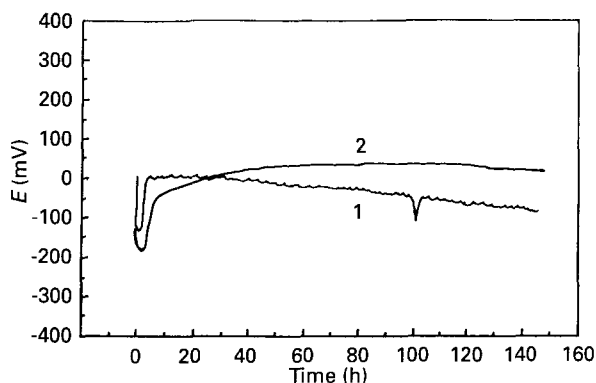


Figure 4 Open-circuit potential versus time measurements (1) original specimen; (2) laser-treated sample.

treated surface. In Fig. 3 one can see a cross-section perpendicular to the feed direction of the X-Y table of a sample showing that voids disappeared in the melted zone at least to 100  $\mu\text{m}$  depth. Fig. 4 gives the long-term (six days) open-circuit corrosion potential,  $E_{\text{corr}} = f(t)$ , curves of specimens with crevice geometry.  $E_{\text{corr}}$  is always more noble for the laser-treated samples. No potential drops, indicative of breakdown

phenomena, occur for laser-treated surfaces, contrary to what is observed for the non-treated material. Therefore, under the experimental conditions used in this work, laser melting is not detrimental in terms of crevice attack over a period of at least 140 h.

Cyclic polarization curves for non-treated and treated samples are given in Figs 5 and 6, respectively. There is no hysteresis loop in the former, while in the latter the cyclic polarization curve shows a very small hysteresis loop. One can consider that the protection potential,  $E_{prot}$ , is equal to the pitting potential,  $E_p$ , and in these conditions both non-treated and laser-treated surfaces present high crevice corrosion resistance [4, 8–10]. This result shows that laser treatment is not detrimental to the Co–Cr–Mo alloy in terms of crevice corrosion resistance. A Bode diagram for the laser-treated samples is given in Fig. 7. Bode diagrams for the non-treated samples are not shown because of their similarity with those in Fig. 7. The results of these studies for the non-treated and laser-treated samples, at  $E_{corr}$ , are given in Table I. The Bode diagrams show that the interface has a resistive behaviour for the high values of applied frequency. Normally, this behaviour is attributed to the resistance of the electrolyte, since the contribution of the passive film is negligible [11–12]. High dispersion has been observed in the  $|Z|$  values for low frequencies. A linear

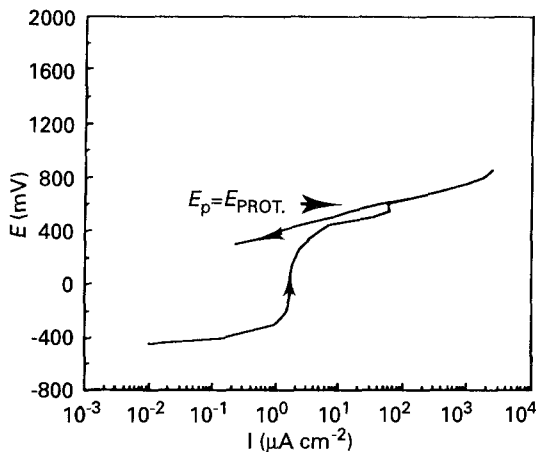


Figure 5 Cyclic polarization of non-treated sample.

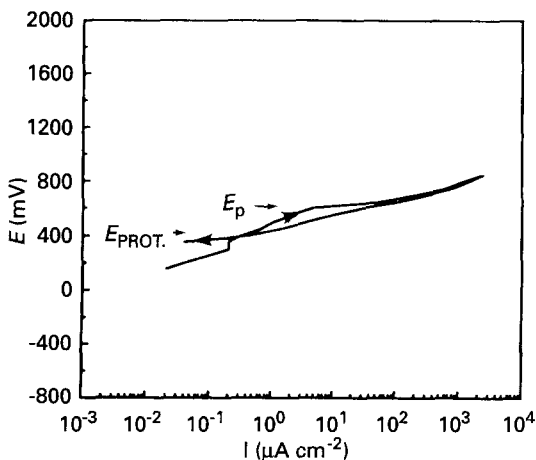


Figure 6 Cyclic polarization of laser-treated sample.

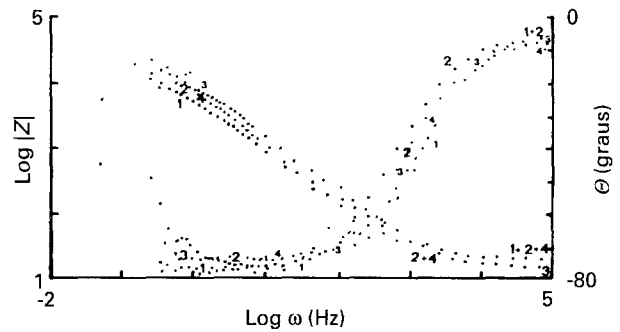


Figure 7 Bode diagram of laser-treated Co alloy.  $Z$ : electrochemical impedance;  $\theta$ : phase angle;  $\omega$ : frequency.

TABLE I Impedance data from Bode–Nyquist spectra

Surface	Slope	Phase angle, $\theta$ (degrees)	Capacitance, $C_{sc}$ ( $\mu\text{F cm}^{-2}$ )
Laser treated	-0.71	-79	797.7
Original	-0.71	-85	11.7

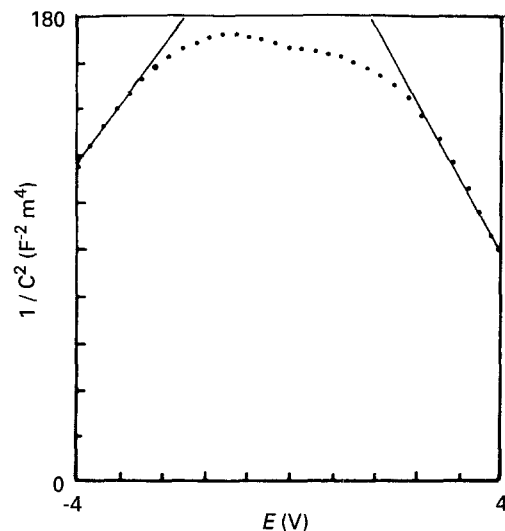


Figure 8 Mott–Schottky impedance spectrum of laser-treated sample.

decrease of  $|Z|$  with increasing frequency may be observed in the intermediate region. Table I gives the slope of the  $\log |Z|$  versus  $\log \bar{\omega}$  plot, the phase angle,  $\theta$ , and the capacitance of the space charge layer,  $C_{sc}$ , after 1 h of immersion and obtained from Nyquist spectra. No significant differences exist in the values of these parameters when the original surfaces are compared with laser-treated surfaces, except for the capacitance of the space charge layer  $C_{sc}$ .

In Fig. 8 is shown a Mott–Schottky plot for laser-treated Co–Cr–Mo alloy. Plots for non-treated specimens are not shown because of their similarity. One can consider that the film has semiconducting properties with a transition from n-type to p-type at higher potential values. Data from these plots are given in Table II for immersions of 1 h before testing. The flat band potential,  $E_{fb}$ , is higher for laser-treated samples than those for non-treated ones, and the same behaviour is observed for the space charge thickness

TABLE II Data from Mott-Schottky impedance spectra

Surface	$E_{fb}$ (mV)	$W$ (nm)	$N_D$ (at $\text{cm}^{-2}$ )
Laser treated	- 832	1.4	$4.1 \times 10^{20}$
Original	- 1085	0.92	$1.4 \times 10^{21}$

$E_{fb}$  – flat band potential;  $W$  – thickness of space charge layer;  $N_D$  – density of donors

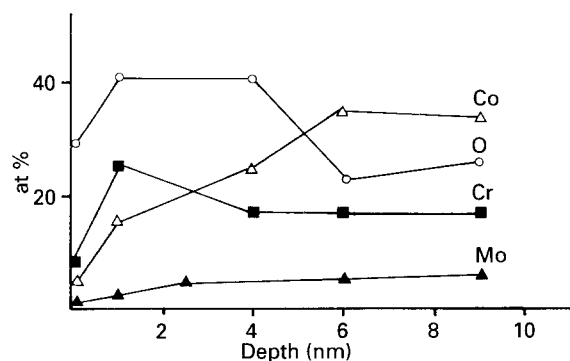


Figure 9 XPS depth profile of laser-treated specimen ( $\Delta$  Co;  $\circ$  O;  $\blacksquare$  Cr + ;  $\blacktriangle$  Mo).

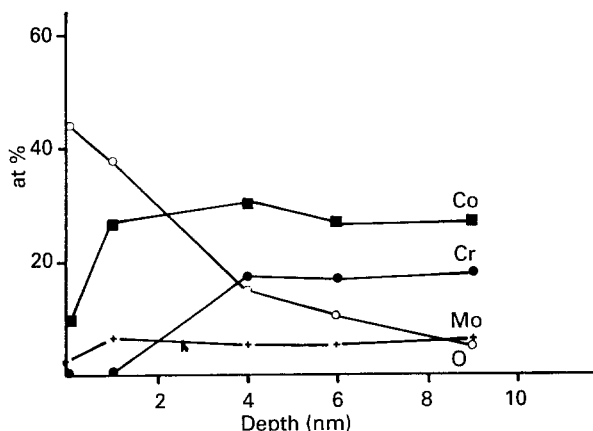


Figure 10 XPS depth profile of origin sample ( $\blacksquare$  Co;  $\bullet$  Cr;  $\circ$  O;  $+$  Mo).

$W$ , while the density of donors,  $N_D$ , is lower. These data constitute evidence that the surface films are different. However, the interpretation of these data is difficult because of the roughness introduced by the laser treatment which increased the true area of the specimens. For these conditions it may be considered that the film on treated specimens is less conductive and slightly more corrosion resistant than the film on non-treated specimens [13].

One can consider that changes in film properties introduced by the laser treatment are not very significant, as shown by the Bode diagrams and the Mott-Schottky impedance data.

In Figs 9 and 10 the XPS depth profiles of laser-treated and non-laser-treated specimens are shown,

respectively. As one can see there is an enrichment in oxygen and a decrease in Cr for laser-treated samples. Analysis of the binding energies has shown that the film is mostly formed by  $\text{Cr}_2\text{O}_3$  and the Co appears to be present in the metallic state (spectra not shown).

#### 4. Conclusions

From this work the following conclusions can be drawn:

1. Both non-treated and laser-treated Co alloys show good crevice corrosion resistance.
2. During polarization of the original samples corrosion occurred in the grain boundaries while for laser-treated samples corrosion occurred at the dendrites that formed during cooling of the material.
3. Surface voids disappeared in the melting zone to a depth of at least 100  $\mu\text{m}$ .
4. Bode-Nyquist and Mott-Schottky experiments have shown that the materials have the same behaviour under our test conditions.
5. Laser treatment is not detrimental to Co alloys in terms of corrosion resistance but modifies the surface film in terms of the amount of Cr and oxygen. Depletion of Cr in the oxide film may be responsible for the hysteresis loop shown in cyclic polarizations.

#### Acknowledgements

JNICT/CNRS scientific convention is gratefully acknowledged.

#### References

1. L. C. LUCAS, R. A. BUCHANAN, J. E. LEMOUR and C. D. GRIFFIN, *J. Biomed. Mater. Res.* **16** (1982) 799.
2. B. C. SYRETT and E. E. DAVIS, *Corrosion* **34A** (1978) 138.
3. P. SÜRY and M. SEMLITSCH, *J. Biomed. Mater. Res.* **12** (1978) 723.
4. B. C. SYRETT, in "The application of electrochemical techniques to the study of corrosion of metallic implant materials", edited by R. Baboion (NACE, 1977) p. 93.
5. R. A. SILVA, M. A. BARBOSA, G. M. JENKINS and I. SUTHERLAND, *Biomaterials* **11** (1990) 336.
6. M. A. BARBOSA, Ph.D thesis, University of Leeds (1980).
7. R. A. SILVA, M. A. BARBOSA, R. VILAR, O. CONDE, M. DA CUNHA BELO and I. SUTHERLAND, *Clin. Mater.* **7** (1991) 31.
8. M. J. MULLER and E. H. GREENER, *J. Biomed. Mater. Res.* **4** (1970) 29.
9. J. R. CAHOON and R. BANDIOPADHYA, *ibid.* **9** (1975) 259.
10. P. SÜRY and M. SEMLITSCH, *ibid.* **15** (1981) 611.
11. U. STIMMING, in "Passivity of metals and semiconductors", edited by M. Froment (Elsevier, Amsterdam, 1983) p. 509.
12. K. LEITNER, J. W. SCHULTZE and U. STIMMING, *J. Electrochem. Soc.* **133** (1986) 1561.
13. R. A. SILVA, M. A. BARBOSA, B. RONDOT and M. DA CUNHA BELO, *Brit. Corros. J.* **25** (1990) 136.